BNL 36817

CONF-8504152--7

HIGH ENERGY NUCLEAR COLLISIONS: PHYSICS PERSPECTIVES+)

BNL--36817

DE85 017511

Helmut Satz

Fakultat fur Physik, Universitat Bielefeld
D-48 Bielefeld, Germany

and

Physics Department, Brookhaven National Laboratory
Upton, New York 11973, USA

Abstract

The main aim of relativistic heavy ion experiments is to study the states of matter in strong interaction physics. We survey the predictions which statistical QCD makes for deconfinement and the transition to the quark-gluon plasma.

+) Introductory talk given at the RHIC Workshop, Brookhaven National Laboratory, April 15-19, 1985.

Research carried out under the auspices of the U.S. Department of Energy

Introduction

With the study of nuclear collisions at very high energies, we hope to enter a new and unexplored domain of physics: the analysis of matter in the realm of strong interactions. We want to understand how matter behaves at extreme densities, what states it will form, and how it will be transformed from one state to another.

To reach a theoretical understanding of this new domain, we have to combine the methods of statistical mechanics and condensed matter physics with the interaction dynamics obtained in nuclear and elementary particle physics. To study it experimentally in the laboratory, nuclear collisions are our only possible tool: we have to collide heavy enough nuclei at high enough energies to provide us with bubbles of strongly interacting matter, whose behavior we can then hope to investigate. What in particular do we want to look for?

Strongly interacting systems at comparatively low densities will presumably firm nuclear or, more generally speaking, hadronic matter. At sufficiently high density, the concept of a hadron, with its intrinsic scale of about one fermi, will lose its meaning, and we expect to find a plasma of quarks and gluons. Separating these two regimes is the deconfinement transition, in which the basic constituents of hadrons become liberated. We want to find experimental evidence for this transition and study the properties of the new, deconfined state of matter. How we might do this, how we can attain sufficiently high energy densities, what features of the transition and the plasma are most suitable for observation, what detectors are the most appropriate - all that will be our main subject at this workshop.

In my perspective, I therefore want to remind you of the general theoretical framework for the analysis of matter in strong interaction physics. Given

QCD as the fundamental theory of the strong interaction, we must formulate and evaluate statistical QCD - and thus obtain predictions for the thermodynamic observables we eventually hope to measure. I will begin by recalling the main physical concepts which lead to deconfinement, sketch the development of statistical QCD and then summarize the results so far obtained in its evaluation. In the last section, I want to address the question of deconfinement at finite baryon number density; this is a topic of crucial important for the experiments beginning next year - and we are now at the verge of obtaining first theoretical results.

The Physics of Deconfinement

In an isolated hadron, quarks and gluons are confined to a color-neutral bound state. Why should this binding be dissolved in dense matter?

From atomic physics, we know two mechanisms to break up a bound state - ionization and charge screening. Ionization is a local phenomenon: by force, one or more electrons are removed from a given atom. Screening, on the other hand, is a collective phenomenon: in sufficiently dense matter, the presence of the many other charges so much shields the charge of any nucleus that it can no longer keep its valence electron in a bound state. When this happens, an insulator is transformed into a conductor (Mott transition[1]). We thus have two possible regimes for atomic matter: an insulating phase, in which the electrical conductivity is very small (thermal ionization prevents it from being zero at non-zero temperatures), and a conductor phase, in which collective charge screening liberates the valence electrons to allow global conductivity. The transition between the two regimes takes place when the Debye radius r_D, which measures the degree of shielding, becomes equal to the radius of the bound state - here the atomic radius r_A. The screening radius r_D depends on the density n and the temperature T of the system, typically in the form $r_D \sim n^{-1/3}$ or $r_D \sim T^{-1}$. Hence the condition

$$r_D(n,T) = r_A \tag{1}$$

defines a phase diagram for atomic matter, as shown in Figure 1. In particular, it also determines a critical density $n_c(T,r_A)$ and temperature $T_c(n,r_A)$ for the transition from insulator to conductor.

Deconfinement in strongly interacting matter is the QCD version of such an insulator-conductor transition.[2] At low density, quarks and gluons form color-neutral bound states, and hence hadronic matter is a color insulator. At sufficiently high density, the hadrons will interpenetrate each other, and the color charge of a quark within any particular hadron will be shielded by all the other quarks in its vicinity. As a result, the binding is dissolved, the colored constituents are free to move around, and hence the system becomes a color conducting plasma. Colors screening thus reduces the interaction to a very short range, suppressing at high density the confining long-range component.

On a phenomenological level, we can then argue just as above that deconfinement will set in when the screening radius becomes equal to the hadron radius,

$$r_D(n,T) = r_H \simeq 1 \text{ fm} . \tag{2}$$

For matter of vanishing baryon number density ("mesonic matter"), this condition[2] leads to a deconfinement temperature of about 170 MeV - a value which agrees remarkably well with that obtained in statistical QCD, as we shall see shortly.

For strongly interacting matter, a counterpart of the electrical conductivity as "phase indicator" emerges if we consider the function[3,4]

$$C(r) = e^{-V(r)/T} , \quad (3)$$

where V(r) denotes the interaction potential between a quark and an antiquark at separation r. In the confinement regime, V(r) rises linearly with r, so that here C(r) should vanish as $r \to \infty$. Actually, it doesn't vanish identically: when V(r) becomes equal to the mass m_H of a hadron, it is energetically favorable to "break the string" by creating a new hadron. Therefore C(r) becomes exponentially small in the large distance limit,

$$C(\infty) \sim e^{-m_H/T} , \quad (4)$$

but it vanishes only for $T \to 0$. In this way, hadron production plays the role of ionization, providing a small local correction to $C(\infty) = 0$.[5] In the deconfined phase, on the other hand, global color screening suppresses any interaction at large r, so that here

$$C(\infty) \sim 1 . \quad (5)$$

The large distance limit of the q-$\bar{q}$ correlation function C(r) thus tells us in which of the two regimes the system is.

After this brief look at the physical concepts underlying the different states of strongly interacting matter, let us see what we can calculate in the framework of statistical mechanics, with QCD as basic dynamical input.

Statistical QCD

QCD describes the interaction of quarks and gluons in the form of a gauge field theory, very similar to the way QCD does for electrons and photons. In both cases we have spinor matter fields interacting through massless vector gauge fields. In QCD, however, the quarks can be in three different color charge states, the gluons in eight. The intrinsic charge of the gauge field is the decisive modification in comparison to QED; it allows the gluons to interact directly among themselves, in contrast to the ideal gas of photons, and it is this interaction which leads to confinement.

The Lagrangian density of QCD is given by

$$\mathscr{L} = -\frac{1}{4} F^a_{\mu\nu} F^{\mu\nu}_a - \sum_f \bar{\psi}^f_\alpha (\not{\partial} - g\not{A})^{\alpha\beta} \psi^f_\beta \ , \qquad (6)$$

with

$$F^a_{\mu\nu} \equiv (\partial_\mu A^a_\nu - \partial_\nu A^a_\mu - g f^a_{bc} A^b_\mu A^c_\nu) \ . \qquad (7)$$

Here A^a denotes the gluon field of color a ($a = 1,\ldots,8$) and ψ^f_α the quark field of color α(α = 1,2,3) and flavour f. We shall need here only the essentially massless u and d quarks; the others are much more massive and hence thermodynamically suppressed at non-zero temperature. The structure constants f^a_{bc} are fixed by the color gauge group SU(3); for f = 0, the Lagrangian (6) would simply reduce to that of QED, with no direct interaction among the gauge field particles.

Equation (6) contains one dimensionless coupling constant g, and hence provides no intrinsic scale. As a result, QCD only predicts the ratios of physical quantities, not absolute values in terms of physical unit.

Once the Lagrangian (6) is given, the formulation of statistical QCD is at least in principle a well-defined problem. We have to calculate the partition function

$$Z(T,V) \equiv \mathrm{Tr}\{e^{-H/T}\} \ , \qquad (8)$$

where the trace runs over all physical states in a spatial volume V. From Z(T,V) we can then calculate all thermodynamic observables in the usual fashion.

In practice, the evaluation of eq. (8) encounters two main obstacles. Perturbative calculations lead to the usual divergences of quantum field theory; we thus have to renormalize to obtain finite results. Moreover, we want to study the entire range of behavior of the system, from confinement to asymptotic freedom - i.e., for all values of the effective coupling. This is not possible perturbatively, so that we need a new approach for the solution of a relativistic quantum field thepry. It is provided by the lattice regularization.[6] Evaluating the partition function (8) on a lattice where points are separated by multiples of some spacing a, we have 1/a and 1/(Na) as largest and smallest possible momenta; here Na is the linear lattice size. Hence no divergences can occur now. It is moreover possible to write the lattice partition function in the form for a generalized spin system, which can then be evaluated by a standard method from statistical physics: by computer simulation. The partition function (8) on the lattice becomes

$$Z(N_\sigma,N_\tau,g) = \int \prod_{links} dU\, e^{-S(U,g)} , \qquad (9)$$

where the gauge group elements $U \in SU(3)$ play the role of spins sitting on the connecting links between adjacent lattice sites. The number of lattice sites in discretized space and temperature is denoted by N_σ and N_τ, respectively; the Lagrangian density (6) leads to the lattice action S(U,g), with the coupling g.

The lattice only serves as a scaffolding for the evaluation, and we must therefore ensure that physical observables are independent of the choice of lattice. Renormalization group theory tells us that this is the case if the lattice spacing a and the coupling g are suitable related; for small spacing a, one finds

$$a\Lambda_L \sim \exp\{-\text{const.}/g^2\} \ , \qquad (10)$$

with Λ_L as arbitrary lattice scale. Using this relation, we have for each value of g in eq. (9) a corresponding lattice spacing a; this in turn fixes the volume $V = (N_\sigma a)^3$ and the temperature $T = (N_\tau a)^{-1}$. Thus if we can calculate $Z(N_\sigma, N_\tau, g)$, then we have also the wanted physical partition function Z(T,V), from which we can derive all thermodynamic observables and determine the phase structure of strongly interacting matter.

The Thermodynamics of Quarks and Gluons

The lattice form (9) of the QCD partition functon can, as we had already mentioned, now be evaluated by computer simulation techniques, developed in condensed matter physics.[7] To do this, we begin by storing in a computer the parameters needed to specify the complete state of the lattice system: for each of the $4N_\sigma^3 N_\tau$ links, we have a generalized spin U, parameterized by eight "Euler angles" for color SU(3). For $N_\sigma \sim 10$-20, $N_\tau \sim 3$-5, that means 10^5-10^6 variables; this uses up the memory of the computers so far available for such work, and hence calculations were generally performed on lattices in the indicated size range. Starting from some fixed initial configuration - e.g., all spins set equal to unity - we now pass link by link through the entire lattice, randomly flipping each sign. If the new value increases the weight $\exp\{-S(U)\}$, we retain it; otherwise, we keep the old. Iterating this procedure[8] a sufficient number of times, we arrive for a given fixed g at stable equilibrium configurations, which we use to measure the thermodynamic observables. Let us now look at the results for the main observables so far calculated.

The energy density of the system is given by

$$\varepsilon = -\left[\partial \ln Z(T,V)/\partial(1/T)\right]_V/V \ . \tag{11}$$

For a plasma of non-interacting massless quarks and gluons, it is given by the generalized Stefan-Boltzmann form

$$\varepsilon_{SB}/T^4 = 37\pi^2/30 \simeq 12 \ ; \tag{12}$$

the constant in eq. (12) is determined simply by the number of degrees of freedom of the constituents. For a gas of non-interacting mesons, on the other hand, we get

$$\varepsilon_H/T^4 \simeq 1\text{-}2 \tag{13}$$

by considering as constituents π, ρ and ω mesons with their corresponding masses and charge states. How does the energy density of the interacting QCD system compare to these ideal gas limits?

The results of the complete simulation[5] are shown in Figure 2, together with those for the ideal plasma and the ideal meson gas. We see that when we increase the temperature of the system, the energy density indeed undergoes a rather abrupt transition from values in the meson gas range to values near the ideal quark-gluon plasma. How can we be sure that this is inded the deconfinement transition?

From our above discussion of deconfinement physics we recall that the large distance limit $C(\infty)$ of the $q\text{-}\bar{q}$ correlation can be used to tell us what phase the system is in. For the quantity $\bar{L} \equiv C^{1/2}(\infty)$ we thus expect a sudden change at deconfinement, from $\bar{L} \sim \exp\{-m_H/2T\}$ in the confinement regime to a much bigger value, approaching unity for high temperature, in the plasma region.

The numerical results[5] are shown in Figure 3; they confirm that the sudden change we had found in ϵ indeed comes from deconfinement.

The third observable we want to consider is connected to a somewhat different phenomenon. We recall that conduction electrons in a metal have a different ("effective") mass than an electron in vacuum or in a hydrogen atom. Such a mass shift inside a dense bulk medium is also expected for quarks, but in the opposite direction. The vanishing bare quark mass in the Lagrangian (6) leads to an effective mass $m_q^{eff} \simeq 300$ MeV for the bound quarks in a hadron and hence also in low density hadronic matter. For the deconfined quarks in sufficiently dense matter, however, we expect $m_q^{eff} \simeq 0$. With increasing temperature we should therefore observe not only the deconfinement transition, but also somewhere a drop in the effective quark mass. Since the massless quarks in the Lagrangian (6) imply chiral symmetry for the system, this symmetry must be spontaneously broken at low and then restored at high temperatures. Is the associated chiral symmetry restoration temperature T_{CH} the same as the deconfinement temperature T_c? To test this; we can calculate the quantity $\langle\bar{\psi}\psi\rangle$, which provides a measure of the effective quark mass. In Figure 4, the result is compared to that for the deconfinement measure $\bar{L}$. We see that the two phenomena indeed occur at the same point.

We can thus summarize: QCD thermodynamics predicts that strongly interacting matter will form a hadron gas at low temperatures and a plasma of quarks and gluons at high temperatures. Separating the two regimes is a transition region, where color becomes deconfined and chiral symmetry restored.

To obtain the transition temperature $T_C = T_{CH}$ in physical units, we must fix the arbitrary lattice scale Λ_L by calculating some measured quantity, such as the mass of the proton or the ρ, in the same units. Present results for this lead to a critical temperature of about 200 Mev - in general agreement with an introductory phenomenological considerations. This temperature implies an energy density of about

$$\varepsilon_c \simeq 2.5 \text{ GeV/fm}^3$$

as threshold value for plasma formation.

Critical Behaviour in Dense Baryonic Matter

So far, we have considered the behavior of strongly interacting matter at vanishing baryon number density - simply because this is the case which was generally studied in lattice work up to now. Eventually, however, we want the full phase diagram predicted by QCD - i.e., the analog of Figure 1, with the baryon number density n_B replacing the charge density n. Such a full phase diagram may well exhibit a richer structure than that suggested by the $n_B = 0$ results.

When color screening dissolves the local bonds between the quarks and gluons in a hadron, then the new state of matter need not be one of unbound constituents. It is possible that another state with some new kind of collective binding is energetically more favorable; a well-known example are the Cooper pairs in a superconductor. In our case, gluons could "dress" a quark to keep it massive even beyond deconfinement; this would occur if at low temperatures the transition points for deconfinement and chiral symmetry do not coincide. The resulting phase diagram is shown in Figure 5: between hadronic matter and the plasma there is now an additional intermediate phase, consisting of massive but deconfined quarks. A further increase in density or temperature would eventually drive this constituent quark gas into the final phase of massless quarks and gluons.

A comparative study of deconfinement and chiral symmetry restoration at finite baryon number density is thus clearly of great interest - both experimentally and in statistical QCD. I therefore want to close this perspective with some very recent results[9] on deconfinement at $n_b \neq 0$.

For non-vanishing baryon number density, the parition function (8) is replaced by

$$Z(T,\mu,V) \equiv Tr\{e^{-(H-\mu N)/T}\} , \tag{9}$$

where N/3 is the net baryon number of the system and μ the corresponding "chemical" potential. From eq. (9) we obtain

$$n_B = (T/3V)(\partial \ln Z/\partial \mu)_{T,V} \tag{10}$$

for the overall baryon number density. We thus can now calculate our thermodynamic observables as functions of both T and μ. By studying the deconfinement measure $\bar{L}$, shown in Figure 3 at $\mu = 0$, for different values of μ, we can in particular study how the deconfinement temperature changes when the baryon density is turned on. In Figure 6 we show first results for such a deconfinement phase diagram. The quarks in these calculations were not yet massless - they had the values indicated; nonetheless the results give us some idea of what to expect. We note in particular that for the lightest quarks ($m_q \simeq 20$ MeV), the deconfinement temperature has dropped by about 20% when $\mu \simeq 120\Lambda_L$ - a value roughly equal to that of T_c at $\mu = 0$.

There are also some first results for chiral symmetry restoration at finite chemical potential.[10] They are still for static quarks, however, and do not yet indicate how T_{CH} varies with μ. The quark mass variation of μ_{CH} at fixed T is of the same type as shown in Figure 6. Further work at $\mu \neq 0$ is in progress -

both for deconfinement and for chiral symmetry restoration, and we can expect more conclusive results in the course of this year.

Let me close then by noting that for our new field, the analysis of strongly interacting matter, the main perspective is the prospect: to study and test statistical QCD, to find new states of matter, to simulate the early universe in the laboratory.

References

1) N.F. Mott, Rev. Mod. Phys. 40 (1968) 677.

2) H. Satz, Nucl. Phys. A418 (1984) 447c.

3) L.D. McLerran and B. Svetitsky, Phys. Lett. 98B (1981) 195 and Phys. Rev. D24 (1981) 450.

4) J. Kuti, J. Polónyi and K. Szlachányi, Phys. Lett. 98B (1981) 199.

5) T. Celik, J. Engels and H. Satz, Nucl. Phys. B256 (1985) 670.

6) K. Wilson, Phys. Rev. D10 (1974) 2445.

7) See e.g. K. Binder (Ed.), Monte Carlo Methods in Statistical Physics, Springer Verlag, Berlin-Heidelberg-New York (1979).

8) N. Metropolis et al., J. Chem. Phys. 21 (1957) 1007.

9) J. Engels and H. Satz, Phys. Lett. in press (BI-TP 85/14), May 1985); this work was completed after the meeting.

10) J. Kogut et al., Nucl. Phys. B225 [FS9] (1983) 93.

Figure Captions

Figure 1. Schematic phase diagram for atomic matter, as determined by the electrical conductivity.

Figure 2. The energy density in statistical QCD, compared to an ideal plasma (SB) and an ideal gas of mesons (π, ρ and ω), as functions of $6/g^2 \sim T/\Lambda_L$.

Figure 3. The deconfinement measure $\bar{L}$ as function of $6/g^2 \sim T/\Lambda_L$.

Figure 4. The chiral symmetry restoration measure $\langle\bar{\psi}\psi\rangle$ (open circles) and the deconfinement measure $\bar{L}$ (full circles) as functions of $6/g^2 \sim T/\Lambda_L$.

Figure 5. Scenario for a phase diagram of strongly interacting matter, with an intermediate constituent quark phase (shaded area).

Figure 6. Deconfinement phase diagram, for dynamical quarks of mass $m_q \simeq 400$ MeV (●), 170 MeV (O) and 20 MeV (▲); the curves are only to guide the eye.

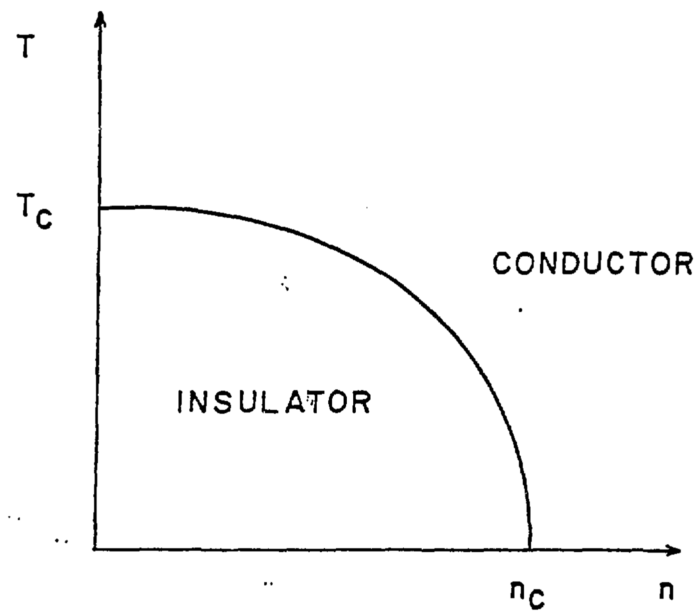

Fig. 1

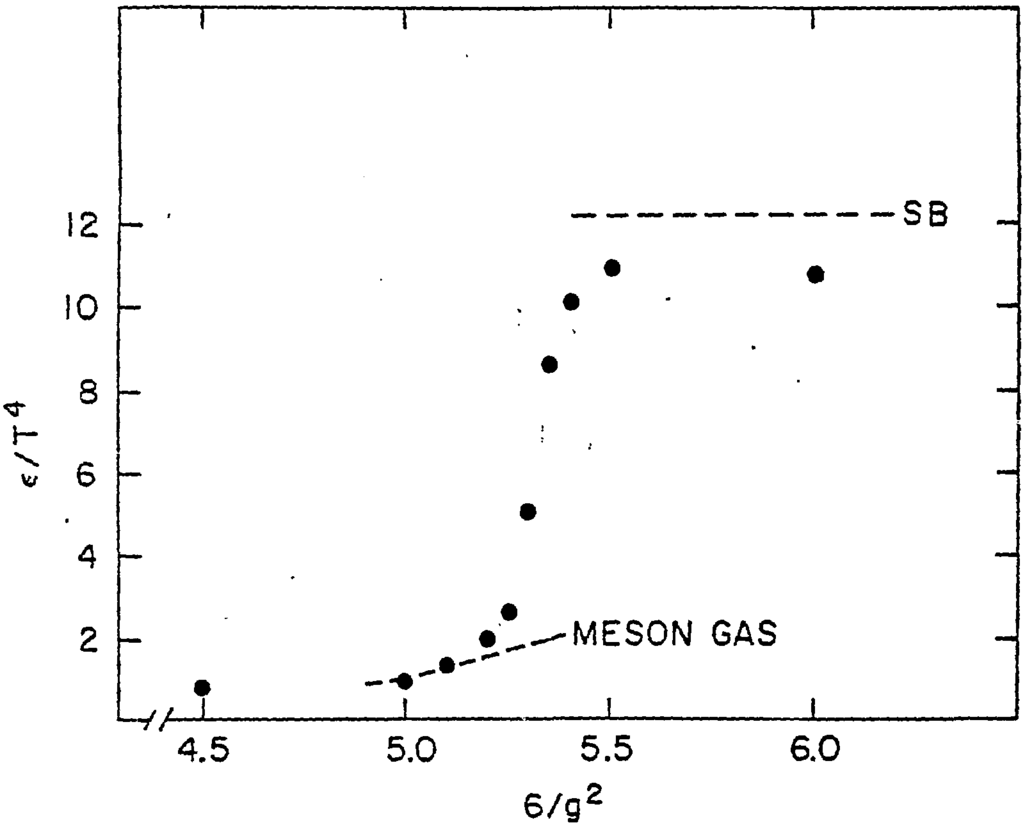

Fig. 2

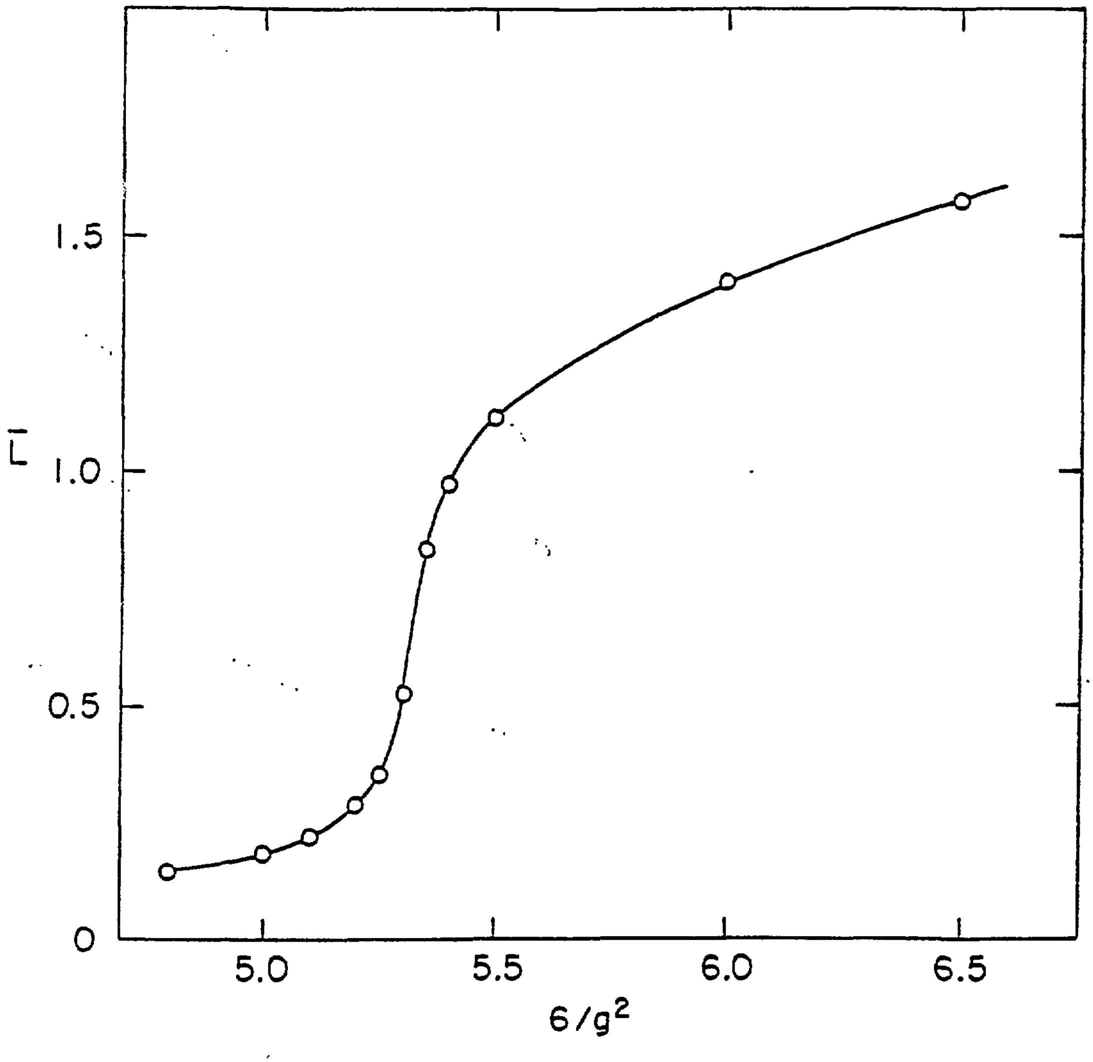

Fig. 3

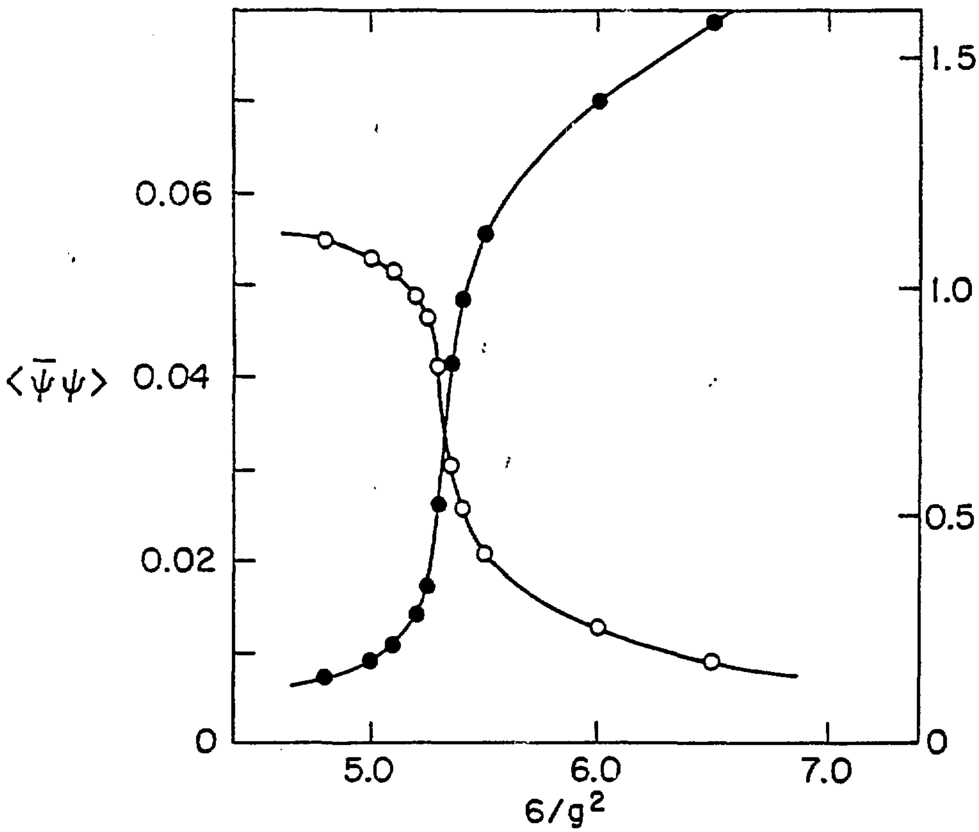

Fig. 4

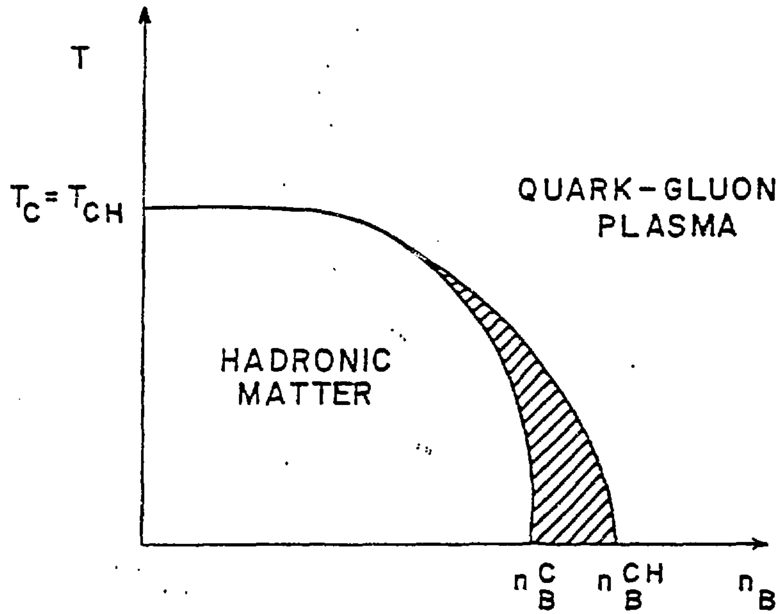

Fig. 5

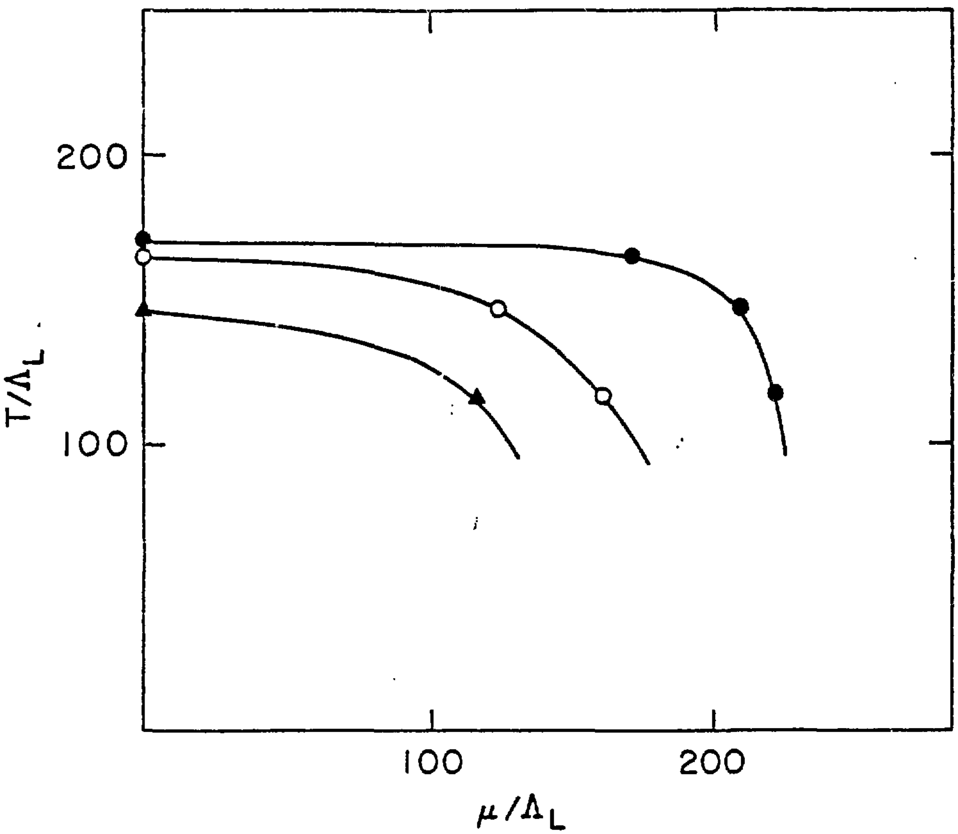

Fig. 6